

observed for incident light at the longer wavelength. Scattering is inversely proportional to the fourth power of the wavelength,<sup>29</sup> therefore, scattering due to surface roughening would be an order of magnitude greater at the shorter wavelength. Apparently, at 1064-nm incident light, enhancement of the SHG due to resonance effects more than compensates for any losses due to scattering.

The small subsequent increases in second harmonic intensity can perhaps also be explained by surface roughening. Boyd and co-workers<sup>25</sup> measured SHG from a variety of metals that had been evaporated onto a roughened glass slide and compared this "surface-enhanced" second harmonic intensity with that from the smooth metal. They found that for nickel, a 20-fold increase in absolute second harmonic intensity could be expected for an incident wavelength of 1064 nm. Since local field enhancement (which is the predominant mechanism for this effect) varies linearly with wavelength,<sup>26</sup> one would anticipate a 10-fold enhancement in SHG for an incident wavelength of 532 nm. It should, however, be noted that the roughened substrate they prepared for their measurements was optimal for surface enhancement; the degree of roughening in this experiment is not controlled; hence, one would not expect to observe such a large effect.

### Summary and Conclusions

SHG, originating at the interface of a nickel electrode in an acidic chloride solution, has been measured. With incident light at a wavelength of 1064 or 532 nm, striking changes in SHG intensity have been observed with the onset of passive film formation. Analyses of the SHG and electrochemical measurements lead us to a number of conclusions.

Passive film formation on polycrystalline nickel in this electrolyte (0.1 M NaCl, 0.01 M HCl) is a two-step process,

(29) Born, M.; Wolf, E. *Principles of Optics*; Pergamon Press: New York, 1970.

as is apparent by the existence of two peaks in the CV. Given the precautions taken to ensure cleanliness, we conclude that the appearance of two peaks at the Ni<sup>+</sup> → Ni<sup>2+</sup> oxidation potential is not due to impurities in the solution.

The dramatic change in SHG ( $\lambda_0 = 1064$  nm) concurrent with the second (more anodic) peak in the CV indicates that actual film formation does not occur until the second of the two peaks. This is consistent with a dissolution-precipitation mechanism for film growth on nickel in this electrolyte, as was originally proposed by Reddy and co-workers.<sup>1-3</sup> SHG intensity for an incident wavelength of 532 nm appears to be primarily influenced by surface roughening.

Future work in this area will involve angularly resolved SHG measurements: by rotating a single-crystal electrode about the surface normal and measuring the variation in second harmonic intensity as a function of the angle of rotation, one should be able to determine the crystal symmetry of the film at the interface giving rise to the SHG.<sup>30-37</sup> Such information should be very useful in further elucidating the structure of the passive film on nickel.

**Acknowledgment.** This work was performed under the auspices of the U.S. Department of Energy, BES-Materials Sciences, under Contract W-31-109-ENG-38.

- (30) Tom, H. W. K.; Heinz, T. F.; Shen, Y. R. *Phys. Rev. Lett.* 1983, 51, 1983.
- (31) Litwin, J. A.; Sipe, J. E.; vanDriel, H. M. *Phys. Rev. B* 1985, 31, 5543.
- (32) Tom, H. W. K.; Aumiller, G. D. *Phys. Rev. B* 1986, 33, 8818.
- (33) Shannon, V. L.; Koos, D. A.; Richmond, G. L. *Appl. Opt.* 1987, 26, 3579.
- (34) Shannon, V. L.; Koos, D. A.; Richmond, G. L. *J. Chem. Phys.* 1987, 87, 1440.
- (35) Robinson, J. M.; Rojantabab, H. M.; Shannon, V. L.; Koos, D. A.; Richmond, G. L. *Pure Appl. Chem.* 1987, 59, 1263.
- (36) Shannon, V. L.; Koos, D. A.; Richmond, G. L. *J. Phys. Chem.* 1987, 91, 5548.
- (37) Shannon, V. L.; Koos, D. A.; Robinson, J. M.; Richmond, G. L. *Chem. Phys. Lett.* 1987, 142, 323.

## Homochiral and Heterochiral Polyesters: Polymers Derived from Mandelic Acid

James K. Whitesell\* and John A. Pojman

Department of Chemistry, The University of Texas at Austin, Austin, Texas 78712

Received July 24, 1989

The kinetics of polymerization of racemic and optically active mandelic acid were determined under a variety of conditions. The initial rate of monomer consumption in the reaction with racemic mandelic acid was approximately twice that for the single enantiomer for acid-catalyzed reactions in benzene solution. A significant increase in the rate of consumption of monomer was observed in the reaction of optically active mandelic acid coincident with the formation of the cyclic dimer (mandelide). The structure of the dimer formed from a single enantiomer of mandelic acid was determined by single-crystal X-ray analysis. These observations are consistent with a scheme where the rate of chain extension of dimeric and higher species is greater than that for the formation of dimers and where the cyclic dimer is derived from trimeric and higher species and not from the noncyclic dimer.

### Introduction

In 1957 Doty reported a fascinating observation on the rates of formation of polypeptides from carbonic anhydride monomers: the rate of polymerization observed for a single enantiomer was approximately 10 times that for the racemate.<sup>1</sup> With simple, second-order kinetics for the

combination of a monomer with a growing peptide, the rate would be reduced by at most a factor of 2 under the scenario where each polymer exhibited a high selectivity for addition of a monomer of the same handedness (or the

(1) Lundberg, R. D.; Doty, P. *J. Am. Chem. Soc.* 1957, 79, 3961-72.

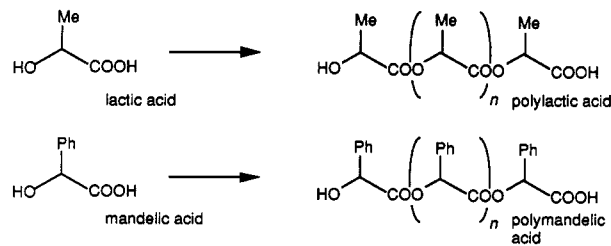


Figure 1.

opposite) as the end with which it was reacting. Since second-order kinetics would not explain the large difference in rate, higher order kinetics must be involved. Doty's observations are consistent (but do not require) a process in which the rate of extension of a chain in a defined (e.g., helical) conformation would be significantly higher than that for less ordered three-dimensional arrangements. A minimum of five monomers all of the same handedness (linked by four peptide bonds) would be required to arrive at a helical conformation at the end of a peptide chain. Such chiral homogeneity would be statistically unlikely unless there were a significant bias for the addition of a monomer of the same handedness as the terminal unit of the growing chain. Indeed, Goodman has shown that the rate of chain elongation of peptides does increase dramatically after an induction period.<sup>2</sup>

These observations have potential implications for a variety of polymers with possible impact in such areas of materials science as optical switches based on nonlinear optical properties where three-dimensional ordering is critical. It is clear that these pioneering studies are worthy of further investigations. However, the study of polypeptides is severely hampered by experimental difficulties, including low solubility of even relatively short-length materials in most solvents. We therefore choose to examine the formation and properties of polyesters derived from optically active hydroxy acids. Certainly, such materials are chemically unique from polypeptides, and information gained from a study of the kinetics of polymerization of hydroxy acids would not necessarily be applicable to an analysis of amino acid polymerization.

Polylactic acid has been studied extensively,<sup>3</sup> in part because of its use as a bioabsorbable material for surgical implants and controlled release of drugs.<sup>4</sup> Further, a recent reports detail investigations of copolymers of lactic acid with other  $\alpha$ -hydroxy acids.<sup>5,6</sup> Unfortunately, lactic acid is relatively easily racemized, making detailed investigations of the influence of handedness on the kinetics of polymerization difficult.<sup>7</sup> On the other hand, we had previously noted that mandelic acid is stereochemically as well as chemically stable under rather drastic conditions of temperature and acidity<sup>8</sup> and thus initiated the study described below (see Figure 1).

### Methods

The formation of polymandelic acid was studied under four sets of conditions: (1) *p*-toluenesulfonic acid (TSA) catalyzed polymerization of mandelic acid in benzene at

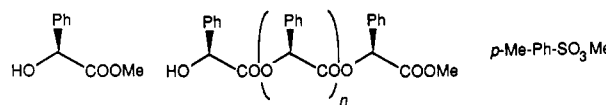


Figure 2.

reflux with azeotropic removal of water; (2) TSA-catalyzed polymerization of mandelic acid in tetrahydrofuran at reflux without removal of water (equilibrating conditions); (3) polymerization of molten mandelic acid; (4) polymerization of molten mandelic acid in the presence of Nafion (a polymeric sulfonic acid resin). In addition, polymerization of a cyclic, condensation dimer of mandelic acid was examined since this species could undergo addition rather than condensation polymerization. A detailed kinetic analysis was possible only in the first case. The reaction mixtures were treated with diazomethane, effecting methylation of mandelic acid and the terminal carboxylic acid groups of the polymeric species forming methyl esters while simultaneously converting the acid catalyst to methyl *p*-toluenesulfonate. Because the acid catalyst was not consumed, the latter species remained constant during the course of the reaction and could be used as an internal standard for HPLC analysis (see Figure 2).

### Experimental Section

**Materials.** Ether and tetrahydrofuran (THF) were distilled prior to use from a deep-blue solution resulting from benzophenone and sodium. Skelly-B was stirred first with concentrated sulfuric acid and then with solid  $\text{Na}_2\text{CO}_3$ , filtered through alumina, and distilled before use. Diazomethane was prepared from Diazald and codistilled with ether prior to use. All other solvents and reagents were used as obtained from commercial sources.

**Procedures.** Reactions in solution were routinely carried out under a nitrogen atmosphere with magnetic stirring. Reactions in the melt were carried out in a vacuum oven thermostated to  $\pm 5$  °C. Preparative chromatography was carried out using recycling techniques with either a Waters Prep-500 system with two normal-phase silica cartridges or a Waters 6000A HPLC pump with two 7.8 mm  $\times$  60 cm Porasil A silica gel columns with a refractive index detector. Analytical HPLC was effected with a Waters 6000A pump and either a Waters Model 440 absorbance detector (254 nm) or with a Waters R401 differential refractometer. A Waters RCM-100 radial compression module housing in  $\mu$ Porasil silica column was used for normal-phase chromatography while gel permeation chromatography was performed using a Waters 500-Å Ultrastryrogel column with THF as the eluting solvent. The relative amounts of compounds were evaluated through the integration of the peak areas by using APPLE INTEGRATOR, a program for the Apple II series produced by Texas Environmental.

**Spectra.** Both carbon NMR and proton NMR spectra were obtained by using a Nicolet NT-360 spectrometer (at 90 and 361 MHz, respectively) with chloroform-*d* as solvent except where indicated. Chemical shift values are reported in ppm downfield from TMS as an internal standard. IR spectra were obtained as KBr pellets by using a Perkin-Elmer 298 infrared spectrophotometer, with polystyrene's absorption at 1601.4  $\text{cm}^{-1}$  as reference. Low-resolution mass spectra in EI mode were recorded using a Bell and Howell Model 21-491 spectrometer at 70 eV. High-resolution mass spectra were recorded with CEC 21-110B instrument in EI mode. Optical rotations were measured with a Perkin-Elmer 141 polarimeter using the sodium D line.

**Kinetics of Esterification of Mandelic Acid with Benzyl Alcohol.** To a 100-mL flask equipped with a Dean-Stark trap and condenser were added 0.151 g (0.79 mmol;  $[\text{H}^+] = 0.16$  M) of  $\text{TsOH}\cdot\text{H}_2\text{O}$ , 0.202 g (1.9 mmol) of benzyl alcohol, 0.291 g (1.9 mmol) of racemic mandelic acid, and 50.0 mL of benzene. The flask was immersed into the oil bath thermostated at 100 °C. Aliquots were removed at various times and derivatized by the dropwise addition of a diazomethane-ether solution until a yellow color persisted. Samples were then concentrated and dissolved in 10 drops of ethyl acetate. Analytical chromatography (4:1 Skelly-B/ethylacetate) was used to determine the relative amounts

(2) Goodman, M.; Peggion, E. *Pure Appl. Chem.* 1981, 53, 699.

(3) Vert, M.; Chabot, F.; LeRay, J.; Chritel, P. *Makromol. Chem. Suppl.* 1981, 5, 30.

(4) Anderson, L. C.; Wise, D. L.; Howes, J. F. *Contraception* 1976, 13, 375.

(5) Fukuzaki, H.; Aiba, Y.; Yoshida, M.; Asano, M.; Kumakura, M. *Makromol. Chem.* 1989, 2407.

(6) Fukuzaki, H.; Aiba, Y.; Yoshida, M.; Asano, M.; Kumakura, M. *Makromol. Chem.* 1989, 2571.

(7) Holten, C. *Lactic Acid*; Verlag Chemie: Weinheim/Bergstr, 1971.

(8) Whitesell, J.; Reynolds, D. *J. Org. Chem.* 1983, 48, 3548.

of methyl mandelate (3.4 column volumes) compared to methyl *p*-toluenesulfonate (2.3 column volumes).

**Preparation of Benzyl Mandelate Oligomers.** To a 1-L flask equipped with a Dean-Stark trap and condenser were added 25.0 g (164 mmol) of (+)-mandelic acid, 6.0 mL (58 mmol) of benzyl alcohol, 3.3 g (17 mmol) of *p*-toluenesulfonic acid hydrate ( $TsOH \cdot H_2O$ ), and 700 mL of benzene. The stirred mixture was heated at reflux for 15 h and then cooled to ambient temperature. Some white material precipitated, and ether was added to achieve a homogeneous solution. The solution was washed once with a 200-mL portion of 2 N aqueous sodium carbonate solution and then with brine and then dried over molecular sieves and concentrated. This material was preparatively chromatographed by using a 5:1 Skelly-B/ethyl acetate solvent system resulting in the recovery of 8.54 g of benzyl mandelate and 6.11 g of benzyl mandelate oligomers. The oligomers were further chromatographed until pure fractions of monomer, dimer, trimer, trimer and tetramer were obtained.

Dimer:  $^{13}C$  NMR 172.7, 167.7, 137.6, 135.0, 133.2, 129.4, 128.8, 128.5, 128.4, 128.3, 127.8, 127.6, 126.9, 75.7, 73.1, 67.2 ppm.

Trimer:  $^{13}C$  NMR 172.4, 167.6, 167.1, 137.6, 135.1, 133.1, 132.8, 129.5, 129.2, 128.7, 128.5, 128.4, 128.2, 127.8, 127.5, 127.0, 75.4, 75.3, 73.2, 67.1 ppm.

Tetramer:  $^{13}C$  NMR 189.2, 172.5, 167.6, 167.0, 137.6, 135.1, 133.1, 132.8, 132.6, 129.5–126.9, 75.4, 75.3, 75.0, 73.2, 67.1 ppm.

**Calibration of UV Detector.** The UV detector was calibrated from samples of benzyl mandelate mixed with known quantities of dimer, trimer, and tetramer. Samples were analyzed by using 4:1 Skelly-B/ethyl acetate. Relative amounts were determined by integration taking into account the length dependence in the extinction coefficient of each oligomer since the absorbing functionality is the benzene ring, of which each molecule has  $x + 1$ , where  $x$  is the number of mandelate residues (the additional benzene ring comes from the benzyl ester).

A mixture of 23.4 mg (0.09 mmol) of monomer and 24.3 mg (0.06 mmol) of dimer was dissolved in ethyl acetate. The mixture was chromatographed three times on a  $\mu$ Porasil column, and the peak areas were integrated and averaged to provide the relative response of the detector. Monomers eluted with 4:1 Skelly-B-ethyl acetate at 2 column volumes, and the dimers, trimers, and tetramers eluted at 2.5, 3.2, and 3.9, respectively. The areas indicated a molar ratio of  $0.9772^{(3/2)} = 1.466$ , where  $^{3/2}$  is the ratio of number of benzene rings. The molar ratio determined from the mass measurements was 1.497, a difference of 2%. The same process was performed with 53.6 mg (0.222 mmol) of monomer and 119 mg (0.233 mmol) of trimer. The calculated molar ratio was 0.962 versus the measured value of 0.9538, a 1% deviation. The final test was performed with 11.4 mg (0.047 mmol) of monomer and 49.1 mg (0.076 mmol) of tetramer, yielding a calculated molar ratio of 0.612 versus the actual value of 0.618 (1% difference).

**Preparation of Methylated Mandelate Oligomers.** The same procedure as in the preparation of benzyl mandelate oligomers was carried out, without benzyl alcohol. Resolved mandelic acid was used. The reaction mixture was methylated by using diazomethane and chromatographed until pure fractions of monomer, dimer, and trimer were obtained.

Methyl mandelate:  $^{13}C$  NMR 174.1, 138.5, 128.6, 128.5, 126.7, 73.0, 52.8 ppm.

Dimer:  $^{13}C$  NMR 172.8, 169.4, 138.7, 134.1, 130.2, 127.6, 76.3, 74.0, 53.6 ppm.

Trimer:  $^{13}C$  NMR 172.6, 168.2, 167.1, 137.6, 133.2, 129.0, 129.6, 127.0, 75.4, 75.3, 73.2, 52.4 ppm.

**Kinetics of Mandelic Acid Polymerization in Solution.** Into a 250-mL flask equipped with a Dean-Stark trap and condenser were added 150 mL of benzene, 0.565 g (2.9 mmol; pH = 1.7) of  $TsOH \cdot H_2O$ , and 2.50 g (16.5 mmol; [mandelic acid] = 0.11 M) of (+)-mandelic acid. Into another 250-mL flask equipped with a Dean-Stark trap and condenser were added 150 mL of benzene, 0.57 g (2.9 mmol; pH = 1.7) of  $TsOH \cdot H_2O$ , and 2.50 g (16.5 mmol; [mandelic acid] = 0.11 M) of (-)-mandelic acid. An oil bath was preheated to 100 °C before both flasks were simultaneously immersed into the bath and a timer started. Samples were taken every 15 min over a 5-h period. The reactions were allowed to proceed for a total of 14 h. Aliquots of 0.5 mL were removed via a 12-in. needle and 1-mL syringe. Hot reaction

solution was repeatedly drawn up into the syringe and expelled until the syringe had reached the solution temperature to prevent precipitation in the syringe barrel. Aliquots were added to a vial and methylated with diazomethane–ether solution. Samples were concentrated and then dissolved in 0.3 mL of ethyl acetate. At approximately 4 h, the (+)-mandelic acid solution became cloudy due to precipitation of the (*S,S*)-mandelide.

The use of the radial compression precolumn enabled samples to be injected directly into the analytical HPLC without pretreatment. With 4:1 Skelly-B/ethyl acetate, methyl *p*-toluenesulfonate eluted at 2.1, methyl mandelate at 4.7, dimer at 6.2, trimer at 9.0, and tetramer at 11.2 column volumes.

**(*S,S*)-3,6-Diphenyl-1,4-dioxane-2,5-dione [(*S,S*)-Mandelide].** To a 300-mL flask equipped with a Dean-Stark trap and condenser were added 15.8 g (100 mmol) of (+) mandelic acid, 0.70 g (3.6 mmol) of  $TsOH \cdot H_2O$ , and 150 mL of benzene. The stirred mixture was heated at reflux for 60 h while initially all the mandelic acid was not soluble. Upon completion, the mandelide was present as a white precipitate. The still-hot reaction mixture was filtered through a glass frit and the filtrate washed with  $CH_2Cl_2$ . The supernatant solution was concentrated to a viscous mass of mandelate oligomers, which was saved for the saponification. The dried filtrate afforded 5.29 g of crude mandelide. GPC analysis revealed  $\approx$ 35% mandelide with the remaining material being polymer shorter in length than 10 units. The mandelide was recrystallized from 1 L of boiling THF to which sufficient  $H_2O$  was added for persistent cloudiness. The solution was allowed to cool to ambient temperature, and the precipitate removed by filtration, affording 1.60 g (11%) of clean mandelide (by GPC), mp 258–259 °C. Optical rotation measurements were made on a sample further purified by vacuum sublimation. The supernatant from the purification was concentrated to yield 2.28 g of material consisting primarily of oligomers and some mandelide.

**Saponification.** The oligomeric material from the reaction was dissolved in 250 mL of THF to which 2.0 g (14.5 mmol) of anhydrous potassium carbonate was added along with 50 mL of  $H_2O$ . The mixture was stirred at ambient temperature for 10 days. An aliquot was removed and acidified to pH < 2 with 2 N aqueous hydrochloric acid. This solution was washed three times with ether, and the organic layer dried over molecular sieves and concentrated. The resulting white material was analyzed by GPC, which revealed the presence of oligomers. All other fractions containing oligomers were added to the  $THF-H_2O-CO_3^{2-}$  reaction solution along with an additional several grams of anhydrous potassium carbonate. The mixture was heated in an oil bath at 45 °C for 3 days. The clear solution was allowed to cool and then acidified as before with 2 N aqueous hydrochloric acid, followed by three 100-mL portions of ether. The ether layer was dried and concentrated, affording 10.7 g of mandelic acid. The mandelic acid was submitted to the same reaction conditions as above for 60 h, yielding an additional 2.0 g of crude mandelide: solubility in acetonitrile,  $K_{sp} = 0.005$  M. Anal. Calcd for  $C_{16}O_4H_{12}$ : C, 71.64; H, 4.51. Found: C, 71.97; H, 4.39. MS 268 ( $M^+$ ), 118, 105, 90, 77, 51; HRMS,  $m/z$  calcd for  $C_{16}O_4H_{12}$  268.0736, found 268.0738;  $[\alpha]_D^{25} -100.8^\circ$  (c 0.12, acetonitrile);  $^1H$  NMR ( $DMSO-d_6$ ) 7.6–7.4 (10 H), 6.59 (s, 2 H) ppm;  $^{13}C$  NMR ( $DMSO-d_6$ ) 166.6 (s), 132.3 (s), 129.3 (d), 128.4 (d), 77.5 (d) ppm; IR 3520, 3080, 3060, 2980, 2940, 1760, 1505, 1460, 1305  $cm^{-1}$ .

**Determination of Equilibrium Constant in THF.** Into a 250-mL oven-dried flask equipped with a condenser were added 100 mL of anhydrous THF, 0.43 g (2.2 mmol; pH = 1.7) of  $TsOH \cdot H_2O$ , and 3.85 g (25.0 mmol) of racemic mandelic acid. The flask was heated in an 80 °C oil bath. After 40 h, an aliquot (0.5 mL) was removed and methylated with diazomethane. After 2 days, the ratio of dimer/monomer was  $0.075 \pm 0.003$ , was determined by analytical HPLC. At this time, an additional 2.16 g (14.2 mmol) racemic mandelic acid was added. Analysis after an additional 4 h showed a monomer/dimer ratio of  $0.070 \pm 0.003$ .

**Melt Polymerization.** In benzene solution, the water formed during the condensation polymerization is removed with a Dean-Stark trap, but in the molten state the water is driven off. Mandelic acid heated above 120 °C melted and began to polymerize without the addition of an acid catalyst. It was not necessary to use a vacuum oven because above 100 °C the water will remain in the gas phase, removed from the molten reaction.

Twenty vials were filled with (+)-mandelic acid and twenty with racemic samples and placed in an oven preheated to 200 °C. Samples were regularly removed and allowed to cool. The samples became progressively darker with an amber color, as time progressed. The average molecular weight (MW) was evaluated by titrating a known mass of polymer to determine the number of moles of acid and necessarily, moles of molecules:

$$\langle \text{MW} \rangle = \text{g/mol of COOH}$$

The mass of a polymer molecule equals the monomer molecular weight plus the number of additional units times the mass of one such unit:

$$\langle x \rangle = (\langle \text{MW} \rangle - 152)/134 + 1$$

**Solution Polymerization with Nafion as Catalyst.** Into a 25-mL flask equipped with a Dean-Stark trap and condenser were added 25 mL of benzene, 2.71 g (2.5 mmol of sulfonic acid groups) of Nafion catalyst beads (Aldrich), and 0.71 g (4.6 mmol) of (+)-mandelic acid. The reaction was heated at reflux for 8 days. The beads turned black, and the solution remained clear. GPC indicated only a small amount of dimer had formed.

**Melt Polymerization with Nafion as Catalyst.** The bottom of a 50-mL Erlenmeyer flask was covered with Nafion beads, and 7.03 g (6.8 mmol) of (+)-mandelic acid was added. The flask was placed into an oven preheated to 180 °C (the beads decompose at a temperature greater than 200 °C). Once each day, the flask was removed and the molten mass stirred with a spatula and a sample removed for GPC analysis. The reaction was followed for a total of 4 days.  $^{13}\text{C}$  NMR 167.1–166.5 (carbonyl), 133–132.5 (ipso), 129.5–127.0 (phenyl), 75.2–74.2 (carbinol) ppm.

**Extent of Decarboxylation during Melt Polymerization with Nafion.** Into a 50-mL single-neck flask was placed 6.37 g (42 mmol) of (S)-(+)-mandelic acid and 4.93 g of Nafion catalyst beads. The flask was sealed with a septum into which and inlet needle for nitrogen and an exit needle were inserted. The flask was heated in an oil bath at 150 °C while a stream of nitrogen was flowed through the flask, and the outflow was bubbled through a 40-mL saturated solution of  $\text{Ba}(\text{OH})_2$  (3.89 M) at 20 °C. After 1 h, a white precipitate had appeared and the reaction was allowed to proceed for 16 h.

The  $\text{BaCO}_3$  was collected by centrifugation and washed with water until the wash was neutral. The  $\text{BaCO}_3$  was dried in a vacuum oven at 130 °C for 24 h. The mass on the  $\text{BaCO}_3$  was 0.176 g (0.89 mmol), corresponding to 2.1% of the theoretical yield.

**Mandelide in Melt Reactions.** Into one vial was added 2.75 g (18 mmol) of (+)-mandelic acid and into another vial was added 1.64 g (11 mmol) of racemic mandelic acid. The vials were heated in an oven at 180 °C for 1 h. GPC indicated only monomers, dimers, and trimers. Both samples were completely soluble in ethyl acetate in which the homomandelide is insoluble. Both samples had essentially identical mass spectra: MS,  $m/e$  268 ( $\text{M}^+$ ), 152 ( $\text{M}^+$ , monomer), 136, 118, 107, 91, 79, 77, 71, 51.

**Titration of Acid Equivalents of Mandelate Polymers.** An approximately 0.015 M solution of sodium methoxide in benzene was prepared according to the procedure of Fritz and Keen.<sup>9</sup> The volume of titrant used was measured with a calibrated 10.0-mL buret. The actual  $[\text{NaOCH}_3]$  was determined by titrating samples of mandelic acid (0.01 g) dissolved in 10 mL of acetonitrile. To serve as an indicator with a yellow color at the equivalence point, 1 drop of a solution consisting of 0.2385 g of 4-phenylazophenol in 100 mL of acetonitrile was added. Approximately 6 mL of titrant were required to achieve the end point. The  $[\text{NaOCH}_3]$  was determined to be  $0.0138 \pm 0.0003$  M for five samples of mandelic acid. Polymer samples were weighed in a 25-mL Erlenmeyer flask, acetonitrile was added, and the solution was titrated with base until a yellow color persisted. Higher average molecular weight samples were more difficult to titrate because the amber color of the material interfered with the observation of the indicator at the end point.

**Kinetics of Melt Polymerization.** Into each of 20 vials (19 × 48 mm) was placed 300 mg of (+)-mandelic acid, and into another set of vials the same was done with racemic mandelic acid. The samples were placed into a vacuum oven preheated to 200

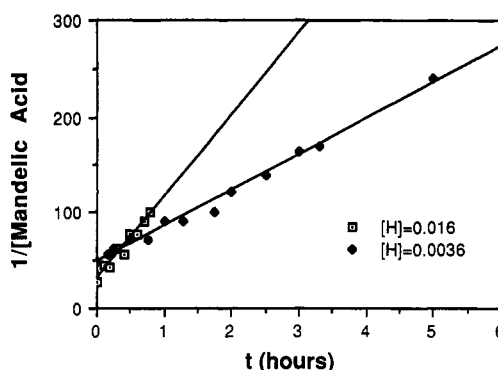


**Figure 3.** Inverse of the mandelic acid concentration plotted against time for two esterifications with benzyl alcohol at different concentrations of acid catalyst. The esterification rate constants, derived from the slope, were  $k_e = 85 \text{ (M}\cdot\text{h})^{-1}$  at  $[\text{TSA}] = 0.016$  and  $k_e = 38 \text{ (M}\cdot\text{h})^{-1}$  at  $[\text{TSA}] = 0.0036 \text{ M}$ . Reaction was performed in refluxing benzene with azeotropic removal of water.

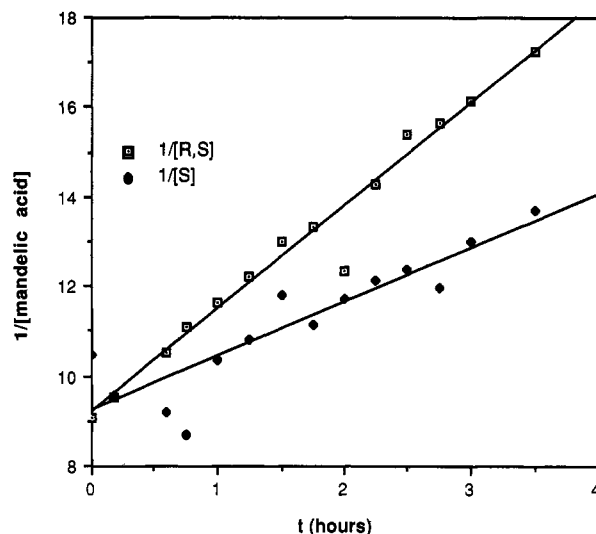


**Figure 4.** Rate of mandelic acid consumption for homo- and heteropolymerization under identical conditions. The derived rate constants for the condensation of racemic mandelic acid was 2.3 versus  $1.2 \text{ (M}\cdot\text{h})^{-1}$  for that of the single enantiomer.

°C. The oven was evacuated with a vacuum pump, although this was later deemed unnecessary. After 1.75 h, the first vial was removed from each set, and this process repeated regularly for 48 h. GPC was performed for each sample, and the average length for the polymers determined by titration.

## Results and Discussion

The kinetics of the esterification of mandelic acid with benzyl alcohol were analyzed first to establish a benchmark for the rates of polymerization as well as to validate the techniques used. Plots of the inverse of mandelic acid concentration are provided in Figure 3 for two reactions using different concentrations of TSA. The rates of esterification derived from the slopes are consistent with half-order behavior with TSA concentration. Other than first-order dependence on [TSA] would be expected as the reactant, mandelic acid, as well as derived polymeric carboxylic acid species would be expected to affect the hydrogen ion concentration.

Self-esterification of mandelic acid as a single enantiomer as well as a racemic mixture was carried out in refluxing benzene with azeotropic removal of water. Analysis of the progress of the polymerization was monitored by the rate of disappearance of mandelic acid (MA). Plots of the inverse of [MA] versus time for both homo- and heterochiral reactions up to 4 h are shown in Figure

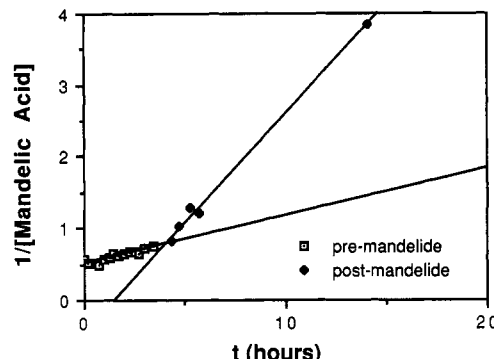


**Figure 5.** Inverse of the mandelic acid concentration plotted for the homocondensation.

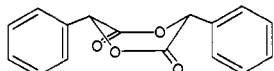


**Figure 6.**

4. The rates of reaction, derived from the slopes of the plots, were  $2.3 \text{ (M}\cdot\text{h)}^{-1}$  for the reaction with racemic (heterochiral) and  $1.2 \text{ (M}\cdot\text{h)}^{-1}$  for the single enantiomer (homochiral) of mandelic acid. Thus, consumption of mandelic acid occurs approximately twice as fast when both enantiomers are present as compared to reaction of homochiral material. This is an inverse relationship to that observed by Doty for the formation of amino acid polymers. In both cases the reactions exhibited smooth, second-order kinetics throughout this time period. Further, it was possible to measure the ratio of hetero- and homodimers formed in the reaction of racemic mandelic acid as the methyl esters of these species were chromatographically resolvable. The relative concentrations of these species was  $1.90 \pm 0.06$ , within experimental error the same as the relative rates of consumption of mandelic acid (1.92) in the hetero- and homochiral polymerizations.

At longer times the rate of consumption of mandelic acid increased markedly. In the reaction with a single enantiomer, the rate constant increased from  $1.2$  to  $5.5 \text{ (M}\cdot\text{h)}^{-1}$  (Figure 5). This observed rate increase is consistent with a scheme where the rate of chain extension of dimeric and longer species is greater than the rate of dimer formation. This kinetic scenario would require the distribution of polymeric species to be different during polymerization than at equilibrium and weighted toward longer chains as the polymerization is proceeding. This is indeed the case, as analyzed by gel permeation chromatography.

The onset of precipitation of the cyclic dimer of mandelic acid was noted at the same time that the rate of consumption of mandelic acid increased. Although this dimer, or mandelide, had been reported previously,<sup>10,11</sup> our observations, including single-crystal X-ray analysis (to be reported elsewhere), represent the first definitive structural proof for this material. The representation of this cyclic dimer shown in Figure 6 is that found in the crystal. This conformational arrangement with a boat form for the bislactone ring is reasonable since it does not involve eclipsing interactions. However, this arrangement may be dictated in part by the presence of hydrogen bonds in the crystal. Molecular mechanics calculations minimize the structure to one with a nearly planar central ring for both the (R,R)- and the (R,S)-mandelide with an insignificant energy difference between the diastereomers. In fact, no

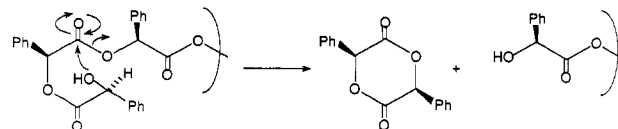


**Figure 7.** Loss of two residues from hydroxyl end of polymer via formation of cyclic mandelide.

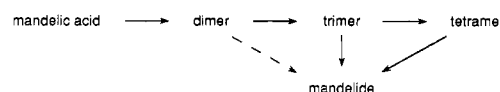
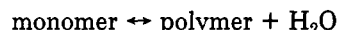


**Figure 8.**

precipitate of either heterochiral or homochiral mandelide was observed in the solution polymerization of the racemic mandelic acid, although the presence of one or both of these species can be inferred from the detection of an ion with the correct mass ( $m/e 268$ ) by mass spectroscopic analysis of the crude reaction solution concentrate, although this observation provides no evidence as to the relative amount of material that was present as mandelide. On the other hand, the presence of substantial quantities of both diastereomeric dimers was confirmed by chromatographic analysis in the polymerization of racemic mandelic acid. Since no precipitate of the highly insoluble, homochiral mandelide was observed during the polymerization of racemic mandelic acid, we conclude that little if any mandelide is derived by the acyclic dimer under these conditions. It is also not likely that the homochiral mandelide formed in the polymerization of homochiral mandelic acid is derived from acyclic dimer.

The lack of formation of cyclic mandelide in the reaction of racemic mandelic acid can be explained if this species was derived from loss of two fragments from the terminal end of trimers and longer polymers (Figure 7). The rate of this process should be affected by the relative stereochemistry of the last two fragments and might also be sensitive to the relative stereochemistry of the third fragment because of the cyclic nature of the transition state (Figure 8). In the polymerization of the single enantiomer of mandelic acid, all species have the same chirality for each of the fragments in contrast to the polymerization of racemic mandelic acid where the probability that the last three fragments have the same handedness is small. In addition to forming mandelide, this process also diverts trimer from conversion to the more reactive, longer oligomers. This accounts for the slower rate of consumption of mandelic acid in the homochiral polymerization where mandelide formation is observed as a significant event.

**Equilibrium Constant.** The mandelic acid condensation equilibrium constant was determined for the following acid-catalyzed reaction in anhydrous THF:



Benzene was not used because the water produced in the reaction would not be soluble. The extent of reaction,  $p$ , was determined from the ratio of the corrected peak areas for monomer and dimer. From the Flory distribution<sup>12</sup>

$$\frac{f(x+1)}{f(x)} = \frac{(1-p)p^x}{(1-p)p^{x-1}} = p$$

the equilibrium constant can be expressed in terms of  $p$ :<sup>13</sup>

$$K = p^2/(1-p)^2$$

(12) Flory, P. J. *Principles of Polymer Chemistry*; Cornell University Press: Ithaca, NY, 1953.

(13) Sawada, H. *Thermodynamics of Polymerization*; Marcel Dekker: New York, 1976.

(10) Whitesell, J.; Reynolds, D. *J. Org. Chem.* 1983, 48, 3548.

(11) Schoberl, A.; Wiegler, G. *Justus Liebigs Ann. Chem.* 1955, 595, 101.

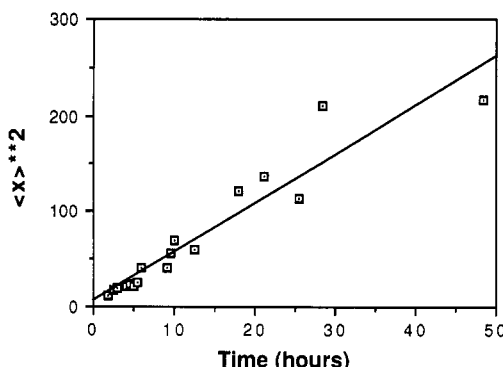


Figure 9. Square of the average length plotted for the uncatalyzed melt polymerization of (+)-mandelic acid at 200 °C.

A value for  $K$  of 0.006 was obtained for the reaction of racemic mandelic acid and *p*-toluenesulfonic acid in THF at 80 °C for 2 days. This extremely small value confirms the necessity for removal of water for a high degree of reaction. The ratio of the dimer diastereomers was very close to unity, indicating that there is little difference in the free energy of hetero- and homodimers.

**Melt Polymerization.** Polyamides have been formed by heating amino acids at a temperature above their melting point,<sup>14</sup> so a similar approach was used with mandelic acid.

If no catalyst is present, then a molecule of mandelic acid can still catalyze the esterification, making the reaction third order. The integrated rate law for a third-order reaction is<sup>15</sup>

$$2C_0k_p t = \langle x \rangle^2 - \text{constant}$$

Figure 9 shows a plot of the square of the average length (determined by titration) versus time for the melt polymerization of (*S*)-(+)-mandelic acid. The slope of the fitted line equals  $2C_0k_p t$  where  $C_0$  is the initial monomer concentration (unity for a pure material) and thus  $k_p = 2.6 \text{ h}^{-1}$ . The poor temperature control ( $\pm 5$  °C) of the oven employed for this experiment contributed to the large data scatter. Within the experimental error, third-order kinetics were confirmed.

The GPC analysis showed that the racemic polymerization had the same retention volume for the maximum of the mass distribution and the same distribution of species. These observations are consistent, within the experimental uncertainties, with the hypothesis that racemic and homochiral mandelic acid polymerize at the same rate in the melt. Likewise, LC analysis revealed that homodimers and heterodimers formed at the same rate.

With the available integrating routine, it was not possible to determine numerical values for the relative distribution of polymer lengths. Nonetheless, information could be gleaned from the range of species present in the distribution as well as the position of the maximum. The qualitative nature of the mass distribution revealed from gel permeation provides information about the relative rates of esterification of mandelic acid versus its oligomers. On the basis of Flory's derivation for polymerization where the rates of all steps are equal, the maximum of the weight distribution ( $x_{\max}$ ) is approximately the same as the average length ( $\langle x \rangle$ ) and given by<sup>12</sup>

$$x_{\max} = \frac{-1}{\log p} \approx \langle x \rangle$$

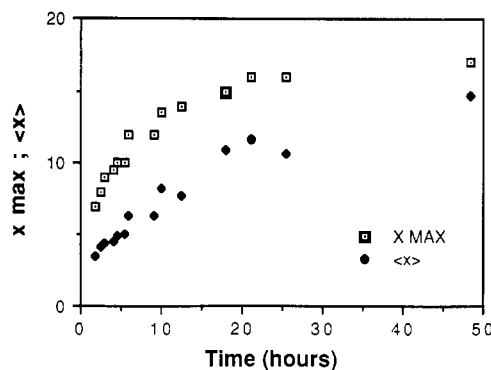


Figure 10.  $x_{\max}$  (determined from GPC) and  $\langle x \rangle$  (determined titrimetrically) are plotted versus time of reaction. The deviation from Flory behavior decreases with time as small oligomers are consumed and the system becomes closer to the Flory distribution.

where  $p$  is the extent of conversion. For the melt polymerization of mandelic acid, the amount of short oligomers is in excess of the weight fraction predicted by the Flory distribution. This is confirmed by comparing the  $x_{\max}$  of the mass distribution plot determined directly by GPC and the actual value of  $\langle x \rangle$  determined by end-group analysis using acid-base titration. Figure 10 presents a comparison of the  $x_{\max}$  from GPC analysis and  $\langle x \rangle$  from titration. As the reaction proceeds, the deviation from the expected Flory behavior diminishes but never disappears. This difference represents an excess of monomer and short oligomers compared to the rest of the distribution, from which it can be concluded that, as with the solution polymerization, the rate of dimer formation from mandelic acid represents the slow step in the polymerization process. Such a dependence of the rate constant on length has been observed for other polycondensation reactions.<sup>15</sup> There were no significant differences in  $x_{\max}$  and  $\langle x \rangle$  values for the polymerization of homo- and heterochiral mandelic acid.

**Nafion Catalysis of Polymerization.** Perfluorinated ion-exchange polymers, with their thermally and chemically stable polymeric backbones and highly acidic sulfonic acid groups, have been used in place of toluenesulfonic acid for organic reactions.<sup>16</sup> Nafion superacid catalyst beads were tested as an esterification catalyst in solution and in the melt. Under conditions similar to those used with *p*-toluenesulfonic acid, mandelic acid did not undergo significant condensation reactions as only a small amount of dimer was detected by GPC. However, in the melt at 180 °C, Nafion beads effectively catalyzed the condensation of mandelic acid. The reaction was so vigorous that gas bubbles were observed streaming out of the molten reaction. After 4 days, the mass distribution had not changed and was uniform throughout the reaction vessel, eliminating the possibility that the reaction could not proceed further because of poor mixing.

The resulting polymer was a very dark, amber color which made titration to determine the average length difficult. However,  $\langle x \rangle$  was estimated to equal approximately 23, the highest value obtained with any polymerization technique. The molten homopolymer could be drawn into brittle, gossamer threads.

**Side Reactions.** There are few side reactions that would be expected to compete with acid-catalyzed esterification leading to polymer formation. Decarboxylation, most likely with concomitant oxidation leading to the

(14) Melius, P. *Biosystems* 1982, 15, 275.

(15) Allcock, H.; Lampe, F. *Contemporary Polymer Chemistry*; Prentice Hall: Englewood Cliffs, NJ, 1981; p 246.

(16) Ford, W., Ed. *Polymeric Reagents and Catalysts*, ACS Symposium Series No. 308; American Chemical Society: Washington, D.C., 1985.

formation of benzaldehyde and carbon dioxide, would consume monomer without producing polymer. A similar decarboxylation could also remove the carboxylic functionality from polymer chains, terminating polymerization from that end and reducing the accuracy of end group analysis by acid-base titration. To ensure that these processes were not a significant factor,  $\text{CO}_2$  production was monitored during polymerization under the most severe conditions—at high temperature in the presence of Nafion. Under these conditions, a maximum of 2.1% of the carboxyl equivalents added as mandelic acid were released as  $\text{CO}_2$ .

**Reactions of the Mandelide.** Tsuruta<sup>17</sup> was able to effect polymerization of the cyclic dimer (lactide) of lactic acid using diethylzinc as an initiator in solution. Attempts on our part to do the same with the mandelide were unsuccessful. Kricheldorf<sup>18</sup> polymerized lactide in solution with various metal alkoxides and noted that these initiators were often effective catalysts for interchange reactions. This too was unsuccessful with the mandelide. Methoxide did initiate polymerization, producing some oligomers from the mandelide, but the average length was much shorter than obtained from the Nafion-catalyzed melt reaction. The length distribution was quite broad, probably as a result of alcoholysis catalyzed by methoxide.

Vert reported<sup>3</sup> the formation of polylactic acid from a zinc-catalyzed ring-opening polymerization in the melt, but similar attempts with the mandelide resulted in thermal decomposition without polymer formation. The high melting point of the mandelide required reaction conditions with temperatures above 250 °C, while the lactide reactions were performed at 140 °C.

### Conclusions

Mandelic acid undergoes condensation polymerization reactions in acid-catalyzed solution as well as in the melt. Linear polyesters were identified and characterized as well as the homochiral cyclic dimer (mandelide). The latter compound appeared as a precipitate in the condensation reaction of a single enantiomer of mandelic acid in benzene with azeotropic removal of water. By contrast, no data confirming the presence of heterochiral dimer in the po-

lymerization of racemic mandelic acid could be obtained. Further, formation of the homochiral cyclic dimer was not observed in the reactions of racemic acid. Since both heterochiral as well as homochiral acyclic dimers were observed to be present in this reaction, it can be concluded that the homochiral, acyclic dimer does not serve as a significant precursor to the homochiral cyclic dimer. By default, then, this cyclic dimer must have been derived from higher oligomers of mandelic acid by loss of two terminal units. Thus, the homochiral, cyclic dimer does not contribute to net polymerization as it is derived itself by a depolymerization process.

The rate of mandelic acid consumption in solution reactions increases sharply with the appearance of oligomers. This is believed to be a result of the loss of intramolecular hydrogen bonding in the monomer that is not possible for oligomers. Thus, mandelic acid reacts more slowly with itself than it does with oligomers, and as a result, the rate of monomer consumption increases as these oligomers form.

Mandelic acid also undergoes self-esterification when heated above its melting point. No stereoselectivity was observed, and the kinetics followed the third-order rate law as would be expected if a third molecule of mandelic acid was involved as an acid catalyst. The average length was lower than the maximum in the mass distribution determined by GPC from which it can be concluded that the rate of esterification increases with length in the melt polymerization as it does in solution. The highest average length ( $\langle x \rangle = 20$ ) polymers were synthesized by using Nafion superacid catalyst beads.

**Acknowledgment.** We are grateful to the Robert A. Welch Foundation (Grant F-626) for financial support of this research. Technical assistance from, as well as helpful discussions with, Dilip K. Kondepudi are gratefully acknowledged.

**Registry No.** ( $\pm$ )-Mandelic acid, 611-72-3; benzyl alcohol, 100-51-6; (+)-mandelic acid, 17199-29-0; *p*-toluenesulfonic acid hydrate, 104-15-4; (+)-benzyl mandelate (dimer), 126296-70-6; (+)-benzyl mandelate (trimer), 126296-71-7; (+)-benzyl mandelate (tetramer), 126296-72-8; (+)-methyl mandelate (dimer), 21210-43-5; (+)-methyl mandelate (trimer), 126296-73-9; (+)-methyl mandelate (tetramer), 126296-74-0; (-)-mandelic acid, 611-71-2; (*S,S*)-mandelide, 126296-68-2; (+)-mandelic acid (homopolymer), 126296-75-1; (+)-mandelic acid (SRU), 126451-97-6; ( $\pm$ )-mandelic acid (homopolymer), 124785-20-2; ( $\pm$ )-mandelic acid (SRU), 124824-89-1.

(17) Tsuruta, T.; Matsuura, K.; Inoue, S. *Markomol. Chem.* 1964, 75, 211.

(18) Kricheldorf, H.; Berl, M.; Scharnagl, N. *Macromolecules* 1988, 21, 286.